ELSEVIER

J. Non-Newtonian Fluid Mech. 85 (1999) 257–271

Journal of Non-Newtonian Fluid Mechanics

Natural convection of a viscoelastic fluid with deformable free surface

L.A. Dávalos-Orozco*, E. Vázquez Luis

Instituto de Investigaciones en Materiales, Universidad Nacional Autónoma de México Apartado Postal 70-360, Coyoacan, 04510 México D.F., Mexico

Received 30 September 1998; received in revised form 23 November 1998

Abstract

In this paper, linear overstable convection of a viscoelastic fluid layer with upper deformable free surface is investigated. For the sake of comparison, the corresponding case for nondeformable free surface is also investigated. The Oldroyd's viscoelastic model constitutive equation with relaxation and retardation times is made use of. Calculations are made with the Maxwell's model as a particular case. It is supposed that the lower flat surface is at fixed temperature and that the upper deformable free surface is at fixed heat flux. Two cases are investigated which differ due to the mechanical boundary conditions imposed on the lower flat wall, that is, it may be solid or stress free. It is found, for different values of the Galileo number, that for relaxation times that are large enough the curves of the critical Rayleigh numbers are lower than those of stationary convection and those of overstability of the Newtonian fluid with deformable free surface. When the lower surface is rigid maxima in the curves of criticality against the relaxation time are found. When the lower surface is stress free, jumps and maxima are found in the curves of the critical wavenumber and frequency against the relaxation time. To explain these jumps and maxima, based on results previously reported in the literature, it is shown that gravity acts as an extra body force through the surface deformation, playing a dual role on the stability of the convective viscoelastic fluid layer.

Keywords: Linear analysis; Viscoelastic; Overstable convection; Surface deformation

1. Introduction

Natural convection has been the subject of research since many years due to its importance in the understanding of phenomena appearing in nature and applications. A monograph on this subject is the classical book by Chandrasekhar [1]. This book presents general results on natural convection research made until the beginning of the 1960s. A more recent review is found in the book by Koschmieder [2].

Natural convection under the presence of extra body forces different from gravity has been investigated due to their possible importance as stabilizing effects. For nondeformable surfaces a review is presented by Chandrasekhar [1] and Koschmieder [2]. When the upper and lower rigid

* Corresponding author. Fax: +52-5-616-1201.

0377-0257/99/$ – see front matter
PII: S0377-0257(98)00195-5

boundaries have a fixed heat flux (see Dávalos-Orozco [3] and Dávalos-Orozco and Manero [4]) it has been found that the critical Rayleigh number is very small (in comparison with the case when the fixed temperature boundary conditions are used) and that the critical wavenumber tends to zero. Under these conditions, it is also possible to have an abrupt jump in the critical wavenumber if two extra body forces, rotation and magnetic field, act simultaneously on the fluid layer (see Chandrasekhar [1] and Dávalos-Orozco [3]). This jump has also been found when the convection is overstable [1].

Natural convection in viscoelastic fluids has also been investigated because of the applications these materials have in industry and geophysics. In the linear stability problem of viscoelastic fluids, only overstable convection is investigated because their stationary motion is identical to that of Newtonian fluids. The overstable convection of a Maxwell fluid was investigated by Vest and Arpaci [5] and Sokolov and Tanner [6]. The Oldroyd's model was first fully investigated by Takashima [7] with fixed temperature at both walls and later by Kolkka and Ierley [8] with fixed heat flux at the boundaries. Kolkka and Ierley [8] also clarify the discrepancy found in the results of papers [5,6]. In Ref. [6] the results of the rigid-rigid case are numerically wrong.

Besides, Takashima investigated the overstable convection of viscoelastic fluids under the influence of external forces like rotation [9] and magnetic field [10]. He found that for small adimensional relaxation time and some values of the relaxation and retardation times ratio, with Taylor or Chandrasekhar numbers that are large enough, the critical wave number and frequency have an abrupt jump. This jump in overstability has not been found in Newtonian fluids when both rotation and magnetic fields act separately [1]. Therefore, we note that the jump occurs because of the action of these external fields on the convecting viscoelastic fluid. These two papers will be discussed presently in regard to our results.

The problem of stationary natural convection with surface deformation was first investigated by Isakson and Yudovich [11] and was also reviewed in the monograph by Gershuni and Zhukovitskii [12]. They found that a convecting fluid layer becomes more unstable when its upper free surface is deformable. They show that the critical Rayleigh number decreases with a decrease in the Galileo number G, which represents the restoring force of gravity on the free surface deformation.

The stationary convection of a rotating fluid layer with upper deformable free surface has been investigated by Dávalos-Orozco and López-Mariscal [13] under a number of boundary conditions. They found that for some thermal boundary conditions the critical wavenumber tends to zero. For some values of the Taylor number a sudden jump to a zero critical wavenumber was also found.

The problem of overstability in a convecting fluid layer with upper free deformable surface was first investigated by Benguria and Depassier [14]. They present, but not discuss, the case of the lower rigid surface because all the marginal curves calculated do not satisfy the Bousinesq approximation which states that $R < \mathrm{Pr}\, G$, where R is the Rayleigh number and Pr is the Prandtl number. All their calculations for the case of a lower free surface satisfy this condition and have the interesting characteristic that all the marginal curves have a critical wavenumber which tends to zero and a critical Rayleigh number which tends to 30, for any G and Pr. This is understandable because the viscous effects start to be negligible when the wavelengths are very long and therefore all the curves tend to the same value of R.

In this paper, the linear overstable convection of a viscoelastic fluid layer with upper deformable free surface is investigated. Use is made of the Oldroyd's constitutive model equation which has relaxation and retardation times. Calculations are also made for the Maxwell fluid, as particular case when the retardation time is zero. Two separate calculations are made according to the properties of the lower

surface which may be rigid or stress free. The thermal boundary conditions are set as fixed temperature at the lower flat surface and fixed heat flux at the upper deformable surface. For the sake of comparison of our results with those of Benguria and Depassier [14] the Prandtl number is set to $\mathrm{Pr} = 1$. They found that for these thermal boundary conditions the overstability in a Newtonian fluid appears before direct convection. Furthermore, calculations are made of the corresponding overstable problem in which the viscoelastic fluid layer has two flat nondeformable surfaces. To our knowledge this problem has also not been reported before. For the sake of comparison, the curves of criticality of the nondeformable case will be presented along with those of the deformable one.

The structure of the paper is as follows. In Section 2 the fundamental and linearly perturbed equations with their corresponding boundary conditions are presented. Section 3 is devoted to the results of the solid-free case and of the free-free case. Section 4 is the discussion and conclusions.

2. Equations of motion

The system under investigation is a viscoelastic fluid layer of thickness d parallel to the (x,y) plane, perpendicular to the acceleration of gravity $\vec{g}$ which is parallel to the z-axis. See Fig. 1. The origin of the coordinate system is located at the mean level of the upper surface which is free and deformable. The lower surface of the fluid layer, located at $z = -d$, is flat and may be rigid or stress free. The viscoelastic fluid model used in the calculations is the Oldroyd's constitutive equation.

An adverse temperature gradient A permeates the fluid which first produces an unstable hydrostatic equilibrium. For temperature gradient that is large enough the equilibrium may be broken to begin instability.

The equations of motion in two dimensions will be used. Note that the final equations and boundary conditions shown below are exactly the same as in three dimensions if the vertical component of the velocity is used instead of the stream function used here. In this way, the results will be the same except that instead of $k = k_x$, $k = (k_x^2 + k_y^2)^{1/2}$ should be used. Therefore, the equations are the following:

The continuity equation for an incompressible fluid

$$\nabla \cdot \vec{u} = 0. \tag{1}$$

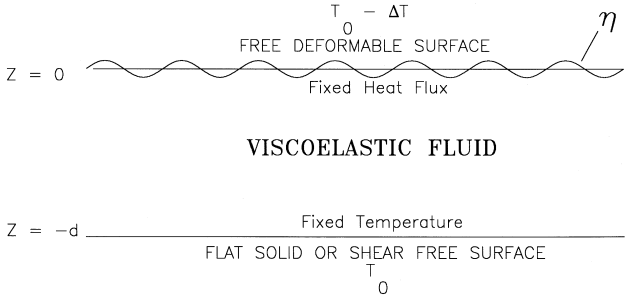

Fig. 1. Sketch of the system under investigation.

The balance of momentum equation in the Boussinesq approximation

$$\rho_0\left[\frac{\partial\vec{u}}{\partial t}+\vec{u}\cdot\nabla\vec{u}\right]=\nabla p+\rho\vec{g}+\nabla\boldsymbol{\tau}. \tag{2}$$

The heat diffusion equation

$$\frac{\partial T}{\partial t}+\vec{u}\cdot\nabla T=\kappa\nabla^2 T. \tag{3}$$

Here, the density depends on temperature as

$$\rho=\rho_0[1-\gamma(T-T_0)], \tag{4}$$

and the viscous stress tensor $\boldsymbol{\tau}$ is related with the shear rate tensor $\boldsymbol{e}$ through the Oldroyd's constitutive equation

$$\boldsymbol{\tau}+\lambda_1\frac{\mathrm{D}\boldsymbol{\tau}}{\mathrm{D}t}=2\rho_0\nu\left(e+\lambda_2\frac{\mathrm{D}e}{\mathrm{D}t}\right) \tag{5}$$

which, in its linear form, can easily be transformed into the general viscoelastic relation of Boltzmann. Here, $\vec{u}$ is the two dimensional velocity vector, p is the pressure, T is the temperature, $\vec{g}$ is the acceleration of gravity parallel to the z-axis, ρ is the density, ρ_0 and T_0 are the constant reference density and temperature, κ is the thermal diffusivity, γ is the coefficient of thermal expansion, $\nu=\mu/\rho_0$ is the kinematic viscosity, μ is the viscosity, and λ_1 and λ_2 are the relaxation and retardation times, respectively. The differential operator D/Dt may be the upper convected, the lower convected or the corotational time derivative. In the linear problem of natural convection this operator becomes the partial time derivative $\partial/\partial t$.

Now, the hydrostatic solution p_s and T_s (see [1]) is perturbed and the new flow variables are $\vec{u}=\vec{v}$, $p=p_\mathrm{s}+p'$, $T=T_\mathrm{s}+\theta$ and $\tilde{\tau}=\tilde{\tau}'$, where $\vec{v}=(u,0,w)$, p', θ and $\tilde{\tau}'$ are the perturbations of velocity, pressure, temperature and viscous stresses. After elimination of the hydrostatic solution they satisfy the following set of equations in a dimensional form:

$$\left(1+\Gamma\frac{\partial}{\partial t}\right)\left(\frac{1}{\mathrm{Pr}}\frac{\partial\vec{v}}{\partial t}-R\theta\hat{k}+\frac{1}{\mathrm{Pr}}\nabla p'\right)=\left(1+\Gamma E\frac{\partial}{\partial t}\right)\nabla^2\vec{v}, \tag{6}$$

$$\frac{\partial\theta}{\partial t}-w=\nabla^2\theta. \tag{7}$$

The pressure may be eliminated if the rotational of Eq. (6) is taken twice. The result of this operation leads to a vector equation for the velocity where the temperature only appears in the z-component. From Eq. (7), we note that merely the z-component of the velocity is necessary to solve the eigenvalue problem. Then, from Eq. (6) after eliminating the pressure, we just need

$$\left(1+\Gamma\frac{\partial}{\partial t}\right)\left(\frac{1}{\mathrm{Pr}}\frac{\partial}{\partial t}\nabla^2 w-R\frac{\partial^2\theta}{\partial x^2}\right)=\left(1+E\Gamma\frac{\partial}{\partial t}\right)\nabla^4 w. \tag{8}$$

Here, $R = g\gamma(-A)d^4/\nu\kappa$ is the Rayleigh number, $\mathrm{Pr} = \nu/\kappa$ is the Prandtl number, Γ is the adimensional relaxation time and E is the retardation and relaxation times ratio. The scaling was made using d, the thickness of the layer, for distance, d^2/κ for time, κ/d for velocity, $-Ad$ for temperature and $\rho_0(\kappa/d)^2$ for pressure. The Laplacian is defined as $\nabla^2 = (\partial^2/\partial x^2) + (\partial^2/\partial z^2)$ and its square ∇^4.

Now, it is necessary to set the boundary conditions for our problem. At the lower surface the mechanical boundary conditions are of two kinds. It may be solid or stress free. Thus, for a solid surface,

$$w = \frac{\partial w}{\partial z} = 0 \quad \text{at} \quad z = -1, \tag{9}$$

and, for the stress free surface,

$$w = \frac{\partial^2 w}{\partial z^2} = 0 \quad \text{at} \quad z = -1. \tag{10}$$

The temperature is fixed at

$$T = T_\mathrm{b} \quad \text{at} \quad z = -1. \tag{11}$$

The upper deformable surface is located at $z = \eta(x,t)$ and has the following boundary conditions. The kinematic boundary condition

$$w = \frac{\partial \eta}{\partial t} + u\frac{\partial \eta}{\partial x} \quad \text{at} \quad z = \eta(x,t). \tag{12}$$

The zero stress jump at the surface

$$(p - p_\infty)n_i = \tau_{ik}n_i, \quad \text{at} \quad z = \eta(x,t), \tag{13}$$

where τ_{ik} is the viscoelastic stress tensor which satisfies Eq. (5). The heat flux is fixed at this boundary

$$\hat{n}\cdot\nabla T = -\frac{F}{(-A)k_\mathrm{T}} \quad \text{at} \quad z = \eta(x,t), \tag{14}$$

where F is the normal heat flux and k_T is the thermal conductivity. The normal and tangent vectors are

$$\hat{n} = \frac{(-\eta_x, 1)}{\mathcal{N}}, \tag{15}$$

$$\hat{\tau} = \frac{(1, \eta_x)}{\mathcal{N}}, \tag{16}$$

where $\mathcal{N} = (\eta_x^2 + 1)^{1/2}$ and the subindexes mean partial derivative. Note that Eq. (14), used when the fluid above the surface is a bad conductor like air, is an approximation because the normal heat flux is assumed constant even though the surface is subject to deformation. In the case of the linear problem all the variables at the deformable surface are expanded in Taylor series around $z = 0$. Thus, to zeroth order, the heat flux is fixed at a flat surface and, consequently, the z derivative of the temperature perturbation will be zero at $z = 0$. See the boundary conditions given below.

From now on, using Eq. (1) we suppose the existence of a current function ψ satisfying $\vec{v} = (\psi_z, -\psi_x)$. In order to linearize the boundary conditions at the upper surface the variables are expanded around $z = 0$ in Taylor series of $\eta(x,t)$. Now, suppose that all the variables are of the form $f = F(z)\exp(ikx + \lambda t)$ (normal modes), where k is the wavenumber, the real part of λ is the growth rate and the imaginary part of λ is the frequency of oscillation. Then, all the equations of motion and boundary conditions become

$$\left(D^2 - a^2 - \frac{N\lambda}{\mathrm{Pr}}\right)\left(D^2 - a^2\right)\Psi = iaNR\Theta, \tag{17}$$

$$\left(D^2 - a^2 - \lambda\right)\Theta = ia\Psi, \tag{18}$$

where $\Psi(z)$ and $\Theta(z)$ are the amplitudes of the stream function and temperature, respectively, and $D = d/dz$. Here $N = (1 + \lambda\Gamma)/(1 + \lambda\Gamma E)$ is a complex constant which depends on the viscoelastic parameters.

From Eqs. (17) and (18) an equation for Ψ alone is obtained

$$\left(D^2 - k^2 - \frac{N\lambda}{\mathrm{Pr}}\right)\left(D^2 - k^2 - \lambda\right)\left(D^2 - k^2\right)\Psi + k^2 NR\Psi = 0. \tag{19}$$

The boundary conditions at the lower surface are for a solid or stress free wall

$$\Psi = D\Psi = 0 \quad \text{at} \quad z = -1, \tag{20}$$

$$\Psi = D^2\Psi = 0 \quad \text{at} \quad z = -1, \tag{21}$$

and for the fixed temperature

$$\Theta = 0 \quad \text{at} \quad z = -1. \tag{22}$$

After making the Taylor expansion around $z = 0$, the boundary conditions for the upper free deformable surface are as follows. The kinematic boundary condition

$$\lambda\eta + ia\Psi = 0 \quad \text{at} \quad z = 0. \tag{23}$$

The conditions for the stresses

$$\left(D^2 + a^2\right)\Psi = \quad \text{at} \quad z = 0, \tag{24}$$

$$\frac{\lambda D^3\Psi}{GN} - \frac{\lambda}{G}\left(\frac{3a^2}{N} + \frac{\lambda}{\mathrm{Pr}}\right)D\Psi - a^2\mathrm{Pr}\Psi = 0 \quad \text{at} \quad z = 0, \tag{25}$$

and the fixed heat flux thermal boundary condition

$$D\theta = 0 \quad \text{at} \quad z = 0. \tag{26}$$

Here, $G = gd^3/\nu^2$ is the Galileo number. From Eq. (25) it is clear the importance G has on surface deformation, it is representative of the restoring gravitational force. When G is very large the boundary condition for a flat surface is recovered. that is, $\Psi = 0$ (see also Eq. (24)).

Suppose a solution $\Psi(z) = \exp(z\alpha)$ in Eq. (19) with α a complex number. Then, α satisfies

$$\left(\alpha^2 - k^2 - \frac{N\lambda}{\mathrm{Pr}}\right)(\alpha^2 - k^2)(\alpha^2 - k^2 - \lambda) + k^2 NR = 0. \tag{27}$$

Therefore, the formal solution for Ψ has the form

$$\Psi = \sum_{i=1}^{3}(A_i \sinh[\alpha_i(z+1)] + B_i \cosh[\alpha_i(z+1)]), \tag{28}$$

where the α_i's are the three main roots of Eq. (27).

Applying the solution Eq. (28) to the boundary conditions Eq. (20) to Eq. (26) and using the solutions for the α_i's we obtain a system of six linear homogeneous equations with six unknowns, the A_i's and B_i's. In order to have a solution different from the trivial one, the 6×6 determinant of this system must be zero. This condition will give the eigenvalues of λ, k and R as functions of the other parameters. From now on, we suppose the marginal oscillatory state where $\lambda = i\sigma_i$, is purely imaginary and σ_i is the frequency.

Two numerical methods of solution are used. The first one is made of two steps. First, with all the other parameters fixed, k and σ_i are given and an initial value of R is used by an algorithm in which Eq. (27) is solved by the Muller Method [15]. Second, the α_i roots are used by the determinant from which a root of R is finally obtained, again, by the Muller method. This root of R has, in general, real and imaginary parts. In order to obtain a real R, new σ_i's are given increasing in small steps (size $\leq 10^{-4}$) until a change in sign in the imaginary part of R is obtained. The corresponding real part is the marginal value of R associated with the k and σ_i. The critical value is obtained changing the magnitude of k in the algorithm explained above and looking for the minimum value of the Rayleigh number. In this way, we obtain the triad R_c, k_c, σ_{ic}, that is, the critical Rayleigh number, wavenumber and frequency.

The other method is based on the use of the approximation proposed by Chandrasekhar [1] and applied with success in his monograph to different problems in hydrodynamic and hydromagnetic instabilities. To our knowledge this method has not been used before in the case of surface deformation.

This method starts proposing an expression for the temperature which satisfies the present boundary conditions, that is: $\theta = \Sigma\, A_m \cos[(m + 1/2)\pi z]$. The algorithm is made in such a way that the Rayleigh number is obtained explicitly. To the zeroth approximation it is obtained directly, but to the first approximation a quadratic equation is obtained which solutions give explicitly two Rayleigh numbers (see [1]). Only that one in agreement with the zeroth approximation was used. In this way, with all the other parameters fixed, for a given k we need to vary the magnitude of σ_i in small steps until the imaginary part of R changes sign and the corresponding real part is the marginal Rayleigh number. Then, changing k, we look for the minimum value of R to obtain the critical triad R_c, k_c, σ_{ic}. This algorithm is very fast and was used instead of the first one. However, the first one, the 'exact' one, was used continuously to check the approximate values of the second. The results were in very good agreement.

These two methods are used for both a viscoelastic fluid layer with upper deformable free surface and for a layer with nondeformable surfaces. The latter, as explained above, has not been calculated before and the results will be used to compare with those of the deformable surface. The next section presents the numerical results.

3. Numerical results

3.1. Lower solid and upper free deformable surfaces

Here, we begin the presentation of the results obtained from the numerical analysis for the solid-free case. Graphs will be presented in order of increasing Galileo number G. The dashed curves will always correspond to the case when both surfaces are nondeformable. Fig. 2, for $G = 100$, shows results of R_c, k_c and σ_{ic} against Γ for different values of E. For this value of G surface deformation is very important. Fig. 2(a) presents curves of R_c against Γ. In the figure two horizontal lines are plotted. One, for $R_{cs} = 669$, corresponds to the critical Rayleigh number for stationary convection. Note that for the present thermal boundary conditions surface deformation is not important in the stationary case (see [13] for the effect of different mechanical and thermal boundary conditions on stationary convection with surface deformation in the presence of rotation). The other one, $R_{on} = 390.8$, corresponds to the critical Rayleigh number for the Newtonian oscillatory convection with deformable surface. The solid curves correspond to the case of upper deformable surface. For all values of E the solid curves are always below the dashed ones. However, the magnitudes of the R_c's approach to each other for large Γ. The Maxwell fluid ($E = 0$, indicated by MAXWELL in the figures) is always the most unstable.

For small Γ's the magnitude of R_c contradicts the condition $R_c < \mathrm{Pr}G$ necessary to satisfy the Boussinesq approximation (see [14]). The reason for this inequality is that, in the present problem, the density and temperature perturbations are related by $\rho = (R/\mathrm{Pr}G)T$ and the Boussinesq approximation is satisfied when the density perturbation is far smaller than the temperature one. However, all the results are presented because it could be possible to observe them, at least in some approximation with our results. The curious property of this curves is that they have maxima above $R_{on} = 390.8$ for small Γ's below 0.1. For very small values of Γ, R_c attains again the value $R_{on} = 390.8$ of the Newtonian fluid.

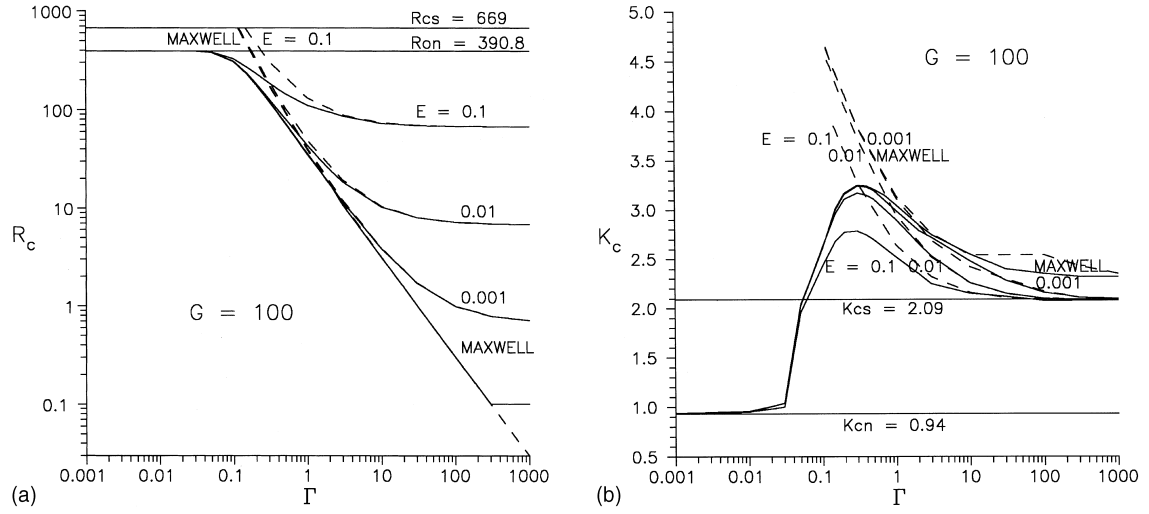

Fig. 2. Solid-free case. Curves of criticality for $G = 100$ and different values of E. The upper deformable free surface case has solid curves and the nondeformable one has dashed curves. (a) R_c against Γ. (b) k_c against Γ.

The maxima are not located exactly at the same Γ but they are around $\Gamma = 0.03$. They have the value of $R_c = 393.19$ for $E = 0.1$, and $R_c = 393.27$ for $E = 0.01$, 0.001, 0 (Maxwell). For Γ's after the maxima the decrease of R_c is monotonic producing more unstable conditions.

Fig. 2(b) shows graphs of k_c against Γ for the same G and different values of E. The dashed curves for the nondeformable case were cut at the value of Γ where R_c crosses the line $R_{cs} = 669$. For reference, two horizontal lines also appear for $k_{cs} = 2.09$ and $K_{cn} = 0.94$. It can be seen that the curves for k_c have maxima. However, for $\Gamma \leq 1$ the Boussinesq approximation is not valid. These maxima are presented with the hope that they could be observed in some approximation. Note that for Γ small k_c tends to k_{cn} but for large Γ it tends to k_{cs}. The curves corresponding to deformable surface are always lower than those of the nondeformable one but they almost have the same value for large Γ. The curves for $E = 0.1$ are lower than the others and the Maxwell fluid has the largest value.

The critical curves of σ_{ic} against Γ are not given here for both cases of lower rigid or free surfaces. An extended version of this paper including this figures may be obtained from the first author upon request.

The critical frequencies tend to $\sigma_{icn} = 4.42$ for small values of Γ. They also have maxima and are surrounded by the curves of the nondeformable surface case. The Maxwell fluid has the largest frequencies and, in all cases for large Γ, they tend to the same value as the nondeformable case and have very small magnitude. It is interesting to note that the maxima of R_c, k_c presented above and that of σ_{ic} do not occur at the same value of Γ but they are near to each other.

Fig. 3 presents results for $G = 250$ and different values of E. Surface deformation is still important for this G. In Fig. 3(a) the curves of R_c against Γ are presented. The solid curves always are below the curves for the nondeformable surface case. The reference line R_{on} is not shown because it is higher than R_{cs} and therefore it is not necessary. With this value of G it is expected to broaden the range of acceptable results inside the Boussinesq approximation and that all those obtained could be observed, even in some approximation for small Γ. The maxima found for $G = 100$ are not shown here

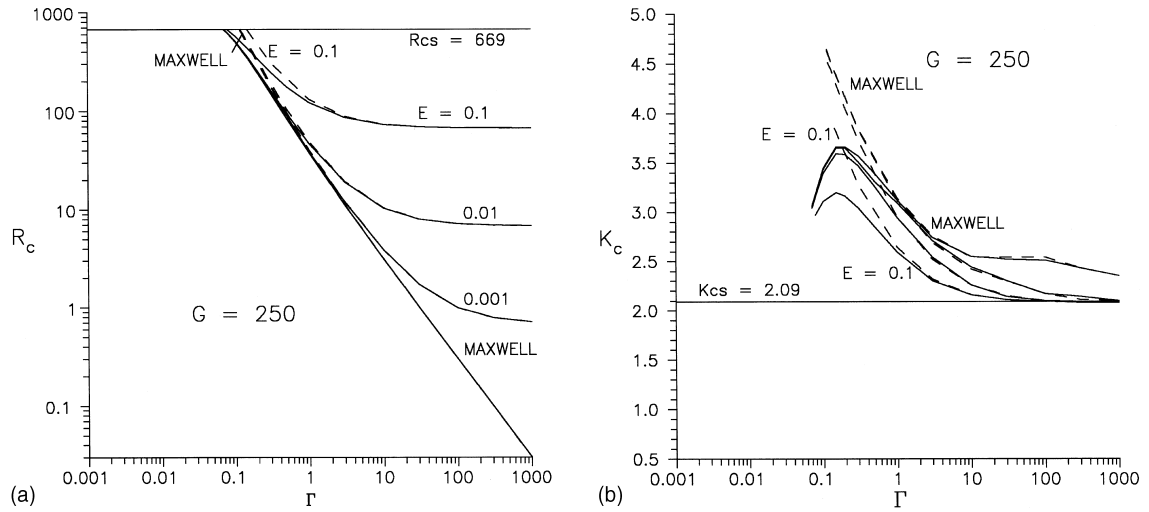

Fig. 3. Solid-free case. Curves of criticality for $G = 250$ and different values of E. (a) R_c against Γ. (b) k_c against Γ.

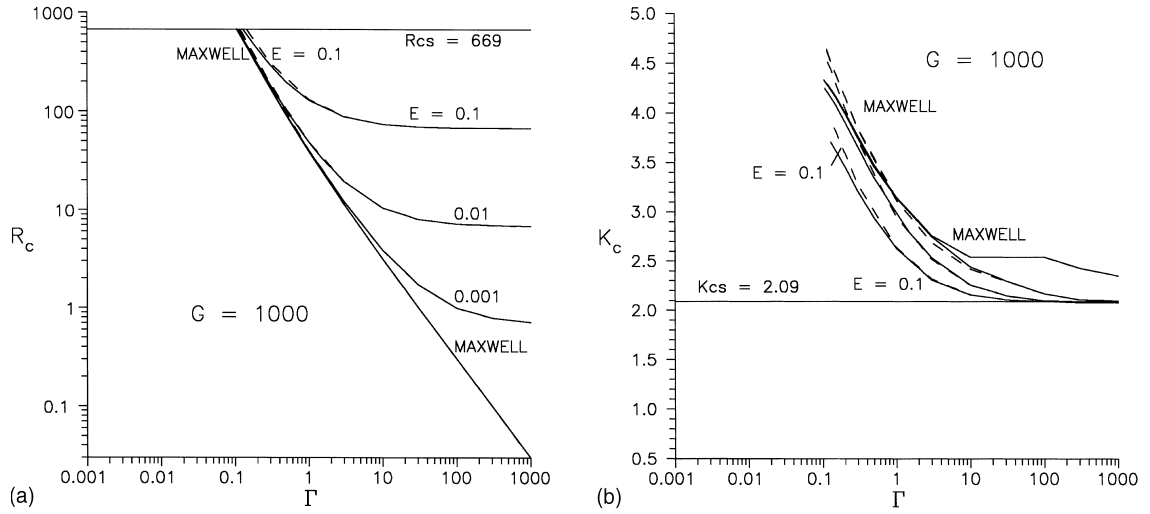

Fig. 4. Solid-free case. Curves of criticality for $G = 1000$ and different values of E. (a) R_c against Γ. (b) k_c against Γ.

because they are above R_{cs}. When Γ is large the R_c's of the solid and dashed curves tend to the same value.

Fig. 3(b) shows graphs of k_c against Γ for the same magnitude of G. Both solid and dashed curves were cut at the Γ where R_c crossed R_{cs}. The solid curves of k_c are always lower than the dashed ones. As explained above, the maxima in the curves of R_c, k_c and σ_{ic} appear for different values of Γ. In this figure it is shown that even though no maxima were accepted for R_c, it is possible to find maxima for the critical wavenumber in all the values of E. For large Γ the critical wavenumber tends to $k_{cs} = 2.09$.

The critical frequencies against Γ are enclosed inside those of the nondeformable case and the frequency values are almost the same except that, here, maxima are also found for the deformable case for small Γ. The Maxwell fluid has the higher frequency which decreases with Γ.

Fig. 4 shows graphs for $G = 1000$ for different values of E. Here, the surface deformation starts to be less important due to the relevant role which gravity begins to have as restoring force at the free surface. In Fig. 4(a) plots are given of R_c against Γ for different values of E. The solid curves are always lower that the dashed ones but they are closer to each other. However, for small Γ the difference is notable but not easily seen in logarithmic scale. For example, for $\Gamma = 0.15$ and $E = 0.1$ in the deformable case $R_c = 569.47$ and for the nondeformable case $R_c = 637.98$ but for $\Gamma = 1$ they are, respectively, $R_c = 129.41$ and $R_c = 131.87$. Again the maxima of this curves are not shown because they are above R_{cs}. All the results presented here may be considered inside the Boussinesq approximation.

Fig. 4(b) presents graphs of k_c against Γ for different values of E and the same G. Here, the critical wavenumbers of the solid curves are below those of the dashed curves for $\Gamma \leq 1$ but are above those of the dashed curves for $\Gamma > 1$. The curves show no maxima because they are in the region where $R_c > R_{cs}$. All the curves tend to k_{cs} for large values of Γ.

The results of the critical frequencies σ_{ic} against Γ for different values of E and the same G show that in both cases the magnitudes are almost the same but, in contrast with Fig. 4(b), maxima are still found in the deformable case for small values of Γ.

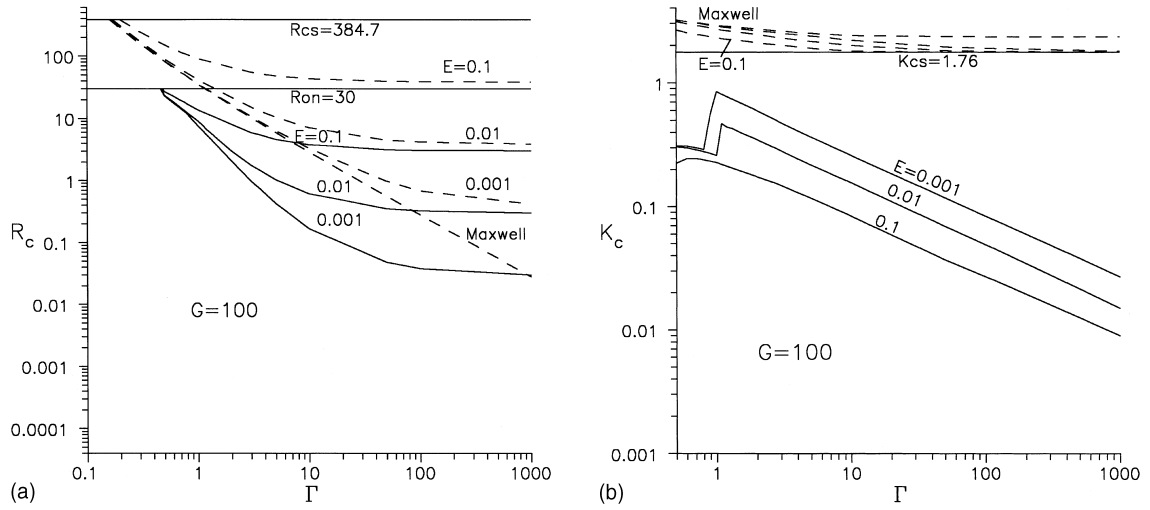

Fig. 5. Free-free case. Curves of criticality for $G = 100$ and different values of E. (a) R_c against Γ. (b) k_c against Γ.

3.2. Lower free and upper free deformable surfaces

In this section numerical results are presented which correspond to a convecting viscoelastic fluid layer with lower flat free surface and upper free deformable surface. The results will be given in order of increasing G. The upper deformable free surface case is shown with solid curves and the upper flat free surface case with dashed curves.

Fig. 5 shows graphs for $G = 100$ and different values of E. In Fig. 5(a) the graphs of R_c against Γ are given. Two horizontal lines are plotted which represent the critical Rayleigh number for stationary convection $R_{cs} = 384.7$ and the critical Rayleigh number for oscillatory convection of a Newtonian fluid $R_{on} = 30$ [14]. Here, in comparison with the previous subsection, the solid and dashed curves separate clearly. It was not possible to calculate the critical curve for the Maxwell fluid for $G = 100$ because the marginal curves were very flat and small numerical oscillations (of one hundredth or one thousandth) in the results prevented us to obtain critical values in a range of k. Another problem was that, when Γ decreases, the magnitude of the wavenumbers in the range where the critical one could be found is so small that the numerical analysis (both methods explained above) do not work very well for the Maxwell fluid with $G = 100$.

Note that, in this case, the marginal curves found are of three kinds. For Γ smaller than a value between 0.4 and 0.5 the marginal curves touch the vertical axis, of the plots of R against k, at $R \to 30$ and the minimum, the critical Rayleigh number $R_c = 30$, corresponds to $k_c \to 0$ (see Fig. 5(a)). For Γ larger than a value between 0.4 and 0.5, but not to large, the marginal curves touch the vertical axis at $R \to 30$ but the minimum $R_c < 30$ corresponds to a finite k_c. Above these, at a certain Γ a jump in the magnitude of k_c is detected. This jump is found due to the form of the marginal curves. That is, they have the form of the greek letter ω with the left side lower than the other one (two local minima) with a small hill in the middle. The left side touches the vertical axis at $R \to 30$. When Γ is increased a little further the left minimum, which was the absolute one, changes places with the second one, and the critical wavenumber increases abruptly. As a consequence of this jump, the critical frequency also

increases abruptly. For larger Γ's, with the left side still touching the vertical axis at $R \to 30$, the second minimum prevails and the critical Rayleigh number decreases monotonically with Γ. The reason why all the curves touch the vertical axis at $R \to 30$ is that the effects of viscosity, and therefore of viscoelasticity, become negligible when $k \to 0$.

The jump in critical wavenumber discussed above is shown in Fig. 5(b) which shows graphs of k_c against Γ for different E and the same G. Note that the jump occurs for viscoelastic fluids with E small and that it is smoothed out for fluids with $E = 0.1$ where a maximum appears around $\Gamma = 0.7$. Notice that, in the graphs, the curves of k_c end at $\Gamma = 0.5$. This is because, as explained above, the critical wavenumber drops to zero ($k_c \to 0$) for Γ's smaller or equal to a value between 0.4 and 0.5.

A similar behaviour occurs for the critical frequency in the results of σ_{ic} against Γ for various values of E. The jumps occur for the same values of Γ as for the critical wavenumber and when $E = 0.1$ the curve has a maximum. When Γ is smaller or equal to a value between 0.4 and 0.5 the critical frequency drops to zero ($\sigma_{ic} \to 0$) along with the critical wavenumber.

The jumps in critical wavenumber and frequency were also found in the papers [9,10] of Takashima. The relation these papers have with our results will be discussed in the next section.

In Fig. 6 shown are numerical results of the case $G = 1000$ for different values of E. Fig. 6(a) gives results of R_c against Γ where we note that the same lines R_{cs} and R_{on} appear again as in Fig. 5(a), in contrast with the solid-free cases discussed in the previous subsection. Here it is possible to show the critical curve for the Maxwell fluid which is the most unstable.

It is important to note that all the critical Rayleigh numbers presented in Fig. 6(a) almost have no difference with those of Fig. 5(a) and Fig. 7(a). Exception made for the Maxwell fluid at large Γ where the magnitude of R_c is very small. Therefore, in the viscoelastic free-free deformable case, the Galileo number G has almost no influence on the instability, except when E is near to zero and Γ is large. This is similar to the Newtonian fluid where $R_c = 30$ is the only critical value for all G. Even though G does not affect the stability too much, it is very important in the change of the critical wavenumber and frequency.

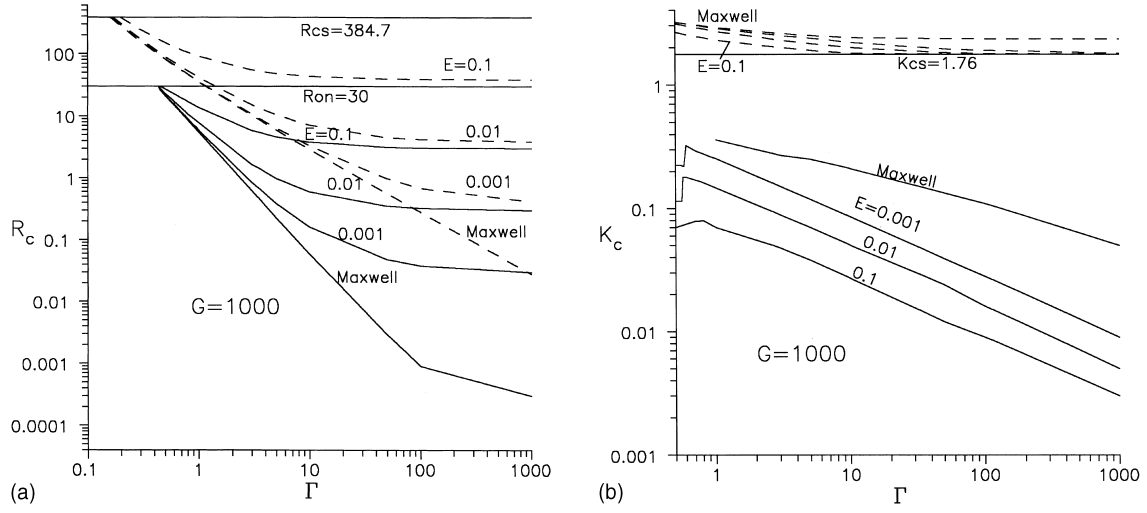

Fig. 6. Free-free case. Curves of criticality for $G = 1000$ and different values of E. (a) R_c against Γ. (b) k_c against Γ.

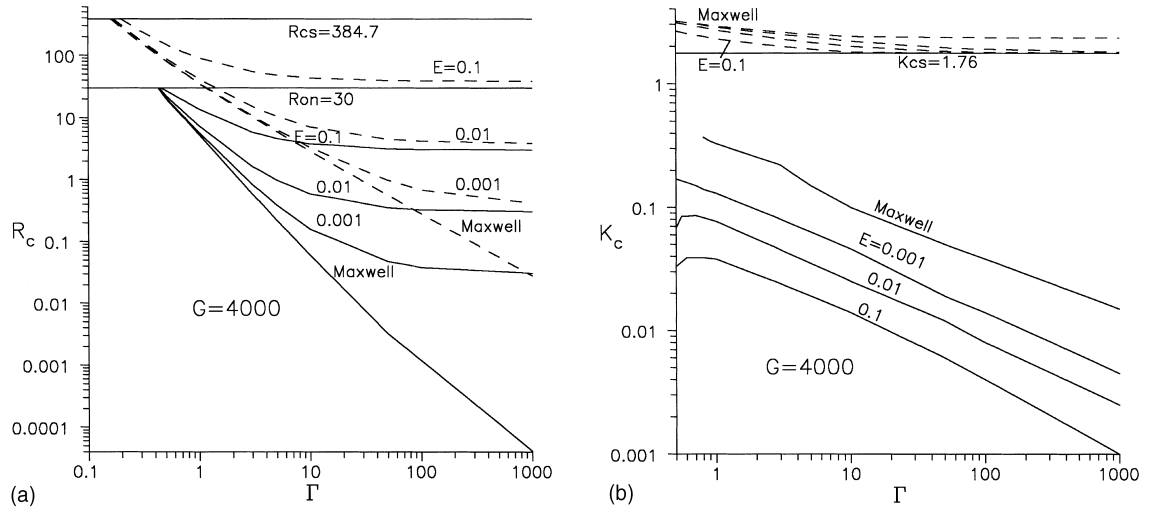

Fig. 7. Free-free case. Curves of criticality for $G = 4000$ and different values of E. (a) against Γ. (b) k_c against Γ.

Comparison of the graphs of k_c against Γ for $G = 100$, 1000, 4000, in Fig. 5(b), Fig. 6(b) and Fig. 7(b), respectively, it is clear that those corresponding to $G = 100$ have the largest k_c's for all values of E. In Fig. 5(b) and Fig. 6(b) found are jumps in the graphs for small values of Γ which are smoothed out for $E = 0.1$. However, when $G = 4000$, as in Fig. 7(b), the jumps are smoothed out into maxima for some values of E. The jump of the curves for the Maxwell fluid were not calculated due to numerical difficulties found at the small wavenumbers.

Comparison of the results of σ_{ic} against Γ for $G = 100$, 1000, 4000, shows that they have almost the same magnitude. The only difference is the place where the jump in frequency occurs. The jump occurs at smaller Γ's when G increases. The jump is smoothed out for some values of E when $G = 4000$.

4. Discussion and conclusions

The increase of degrees of freedom of viscoelasticity makes the fluid more unstable than the Newtonian one. This has been shown in both the solid-free and the free-free cases. In the solid-free deformable case this destabilizing effect of viscoelasticity makes many of the results for the critical Rayleigh number to come inside the Boussinesq approximation when Γ and G increase. In this case, all the critical curves for R_c, k_c, and σ_{ic} against Γ have a maximum. For relatively small G the maxima are outside the Boussinesq approximation and for large G the maxima are above R_{cs}. However, all the results for small G have been presented with the hope that these maxima could in fact be observed with some approximation to our results. In the free-free deformable case all the results are inside the Boussinesq approximation and viscoelasticity destabilizes in a particular way. It makes the marginal curves to change their minimum to a finite critical wavenumber and $R_c < 30$, for Γ that is large enough, while they continue to touch the vertical axis at $R = 30$. In this case, the curves of critical Rayleigh number for any Γ and G are very similar but the convective instability differs in the behavior of k_c and σ_{ic} against Γ. Here, due to the behavior of the marginal curves, a jump in the critical curves of the

wavenumber and frequency is found when Γ increases. This jump is smoothed out into a maximum when increasing E and it disappears for G that is large enough.

The jumps in critical wavenumber and frequency were also found in the papers [9,10] of Takashima. In those papers the convecting viscoelastic fluid is subjected to external body forces different from gravity, like rotation [9] and magnetic field [10]. The results of these papers show that the external forces act on the viscoelastic fluid in such a way that, for certain magnitude of the relaxation time, the size of the convective cell patterns changes abruptly. Moreover, when rotation is present in a viscoelastic fluid, instead of being stabilizing it may be destabilizing for small values of the relaxation times, as shown in Figs. 1(a) and (b) of Ref. [9]. Very similar phenomena have been discussed before for a Newtonian fluid with flat surfaces by Chandrasekhar [1] and Dávalos [3] when rotation and magnetic field interact strongly and for a Newtonian fluid under rotation with deformable surface by Dávalos-Orozco and López-Mariscal (see for example Fig. 13 of Ref. [13]).

The above effects of the extra body forces may be present in our viscoelastic results but now in a new fashion. Here, gravity acts as an extra body force on the viscoelastic fluid through the surface deformation. When this effect is strong, maxima appear in R_c, k_c and σ_{ic} for the solid-free case and jumps and maxima in k_c and σ_{ic} in the free-free case. Here, as in Refs. [9,10], this effect of the dual role of gravity is more important for relatively small Γ.

Among all these new results, general conclusions have been obtained. The results of the solid-free deformable case are more stable than those of the free-free deformable one. The same may be concluded from the results of the nondeformable cases. An increase of the adimensional relaxation time Γ is always destabilizing. An increase in E is stabilizing. An increase in G is stabilizing. For very large Γ the critical values of the deformable and nondeformable cases are very similar (close to each other) but those corresponding to the deformable ones are always more unstable. It is important to take into account that all the stabilizing effects that some of the parameters have on overstability are limited here by $R_c < R_{cs}$.

Acknowledgements

The authors would like to thank support from DGAPA – UNAM to project IN106797. L.A. D-O would also like to thank Mr. Raul Reyes for technical support.

References

[1] S. Chandrasekhar, Hydrodynamic and Hydromagnetic Stability, Oxford University Press, 1961.
[2] E.L. Koschmieder, Bénard Cells and Taylor Vortices, Cambridge University Press, 1993.
[3] L.A. Dávalos O, J. Phys. Soc. Jpn. 53 (1984) 2173.
[4] L.A. Dávalos-Orozco, O. Manero, J. Phys. Soc. Jpn. 55 (1986) 442.
[5] C.M. Vest, V.S. Arpaci, J. Fluid Mech. 36 (1969) 613.
[6] M. Sokolov, R.I. Tanner, Phys. Fluids 15 (1972) 534.
[7] M. Takashima, J. Phys. Soc. Jpn. 33 (1972) 511.
[8] R.W. Kolkka, G.R. Ierley, J. Non-Newtonian Fluid Mech. 25 (1987) 209.
[9] M. Takashima, J. Phys. Soc. Jpn. 33 (1972) 797.
[10] M. Takashima, J. Phys. Soc. Jpn. 33 (1972) 1142.

[11] V.Kh. Izakson, V.I. Yudovich, Izv. An SSSR. Mekh. Zhid. i Gaza 3 (1968) 23.
[12] G.Z. Gershuni, E.M. Zhukovitskii, Convective Stability of Incompressible Fluids, Keter, Jerusalem, 1976.
[13] L.A. Davalos-O, P.G. Lopez-M, Geophys. Astrophys. Fluid Dyn. 80 (1995) 75.
[14] R.D. Benguria, M.C. Depassier, Phys. Fluids 30 (1987) 1678.
[15] D.E. Müller, Mathematical Tables and other Aids in Computation 10 (1956) 208.